JET FLOWS FROM ANGLED NOZZLES

Thomas G. J. Chandler[1] & Philippe H. Trinh[1,2]

[1] Lincoln College, University of Oxford
[2] Mathematical Institute, University of Oxford

UNIVERSITY OF OXFORD

Mathematical problem

In this work, we study the steady-state ejection of a 2D potential fluid (thus incompressible, irrotational, and inviscid) along a semi-infinite channel of width h tilted at an angle γ with the horizontal. As shown in Fig. 1, the jet forms two free-surfaces, and is driven by the influence of gravity and surface tension. In particular, one of our goals is to unify the previous work of Goh and Tuck (1985), treating the case of a horizontal nozzle, with the work of Vanden-Broeck (1984), treating the case of a vertical nozzle. Then, this poster will explore how the angle and configuration of separation depends on the Froude (F) and Weber (α) numbers.

By considering a uniform velocity upstream, the gravity-driven flow is expected to form a vertical jet (see Fig. 1). The system is governed by Laplace's equation, with Bernoulli's equation

$$\frac{1}{2}|\mathbf{u}|^2 + \frac{1}{F^2}(y\cos\gamma - x\sin\gamma) + \frac{1}{\alpha}\mathcal{K} = \text{const.} \qquad [1]$$

on the two free surfaces, for fluid velocity $\mathbf{u}$ and surface curvature $\mathcal{K}$, along with a constant upstream velocity condition and a fixed-wall condition. These boundary conditions are shown in Fig. 1.

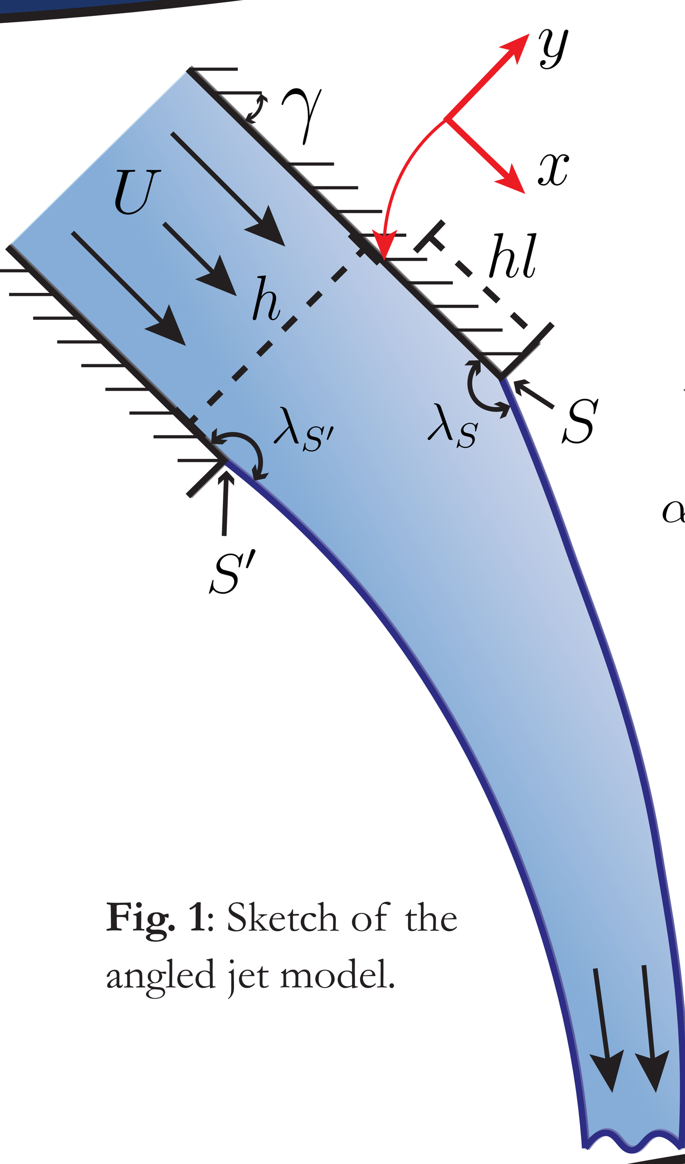

Fig. 1: Sketch of the angled jet model.

Key

U – Unit distance
h – Unit velocity
$F = \dfrac{U}{\sqrt{gh}}$ – Froude number
$\alpha = \dfrac{\rho h U^2}{T}$ – Weber number

$$\phi = \begin{cases} 0 & \text{at } S \\ -\frac{1}{\pi}\log L & \text{at } S' \end{cases}$$

$$\psi = \begin{cases} 0 & \text{at } S \\ -1 & \text{at } S' \end{cases}$$

Analytical results

A local analysis of Bernoulli's equation near the two separation points [c.f. Vanden-Broeck (2010)] shows that, for zero surface tension ($\alpha = \infty$), the upper and lower free-surfaces must separate according to one of three possibilities:

$$\lambda_S = \begin{cases} \frac{2\pi}{3} & \text{for all } \gamma, \\ \gamma & \text{for all } \gamma, \\ \pi & \text{for all } \gamma. \end{cases} \qquad [2]$$

$$\lambda_{S'} = \begin{cases} \frac{2\pi}{3} & \text{for } \gamma \in \left(\frac{\pi}{3}, \frac{\pi}{2}\right], \\ \gamma & \text{for } \gamma \in \left(\frac{\pi}{3}, \frac{\pi}{2}\right], \\ \pi & \text{for all } \gamma. \end{cases}$$

Which scenario will depend on the particular Froude number. In the case of non-zero surface tension ($\alpha \neq \infty$) there is no discrete restriction on the separation angles, and the angle may take some value between $(0, 2\pi)$. In general, this selection mechanism must be determined numerically from the global flow.

Numerical results

The jet is computed by applying a boundary integral method to the free-surface equations and solving for the surface velocities along a stretched grid in the potential plane. Thus at a fixed values of F, L, γ, and α, we are able to determine the jet configuration, including the nozzle overhang, l, and the two separation angles, λ_S and $\lambda_{S'}$ (if they are not already imposed).

In the tensionless case ($\alpha = \infty$), we find there exists two critical Froude numbers, F_U and F_L, for the respective upper and lower free surfaces, which depend on the fixed γ and L values. These critical numbers determine the jet's restricted separation values:

$$\lambda_S = \begin{cases} \pi & \text{for } F > F_U, \\ \frac{2\pi}{3} & \text{for } F = F_U, \\ \gamma & \text{for } F < F_U, \end{cases} \qquad [3]$$

$$\lambda_{S'} = \begin{cases} \pi & \text{for } F > F_L, \\ \frac{2\pi}{3} & \text{for } F = F_L, \\ \gamma & \text{for } F < F_L, \end{cases}$$

with $F_L = 0$ for $\gamma < \pi/3$. In the tension case ($\alpha \neq \infty$), the separation angles are seen to continuously decrease from π (tangential) to γ (horizontal) as F decreases.

Visualisation of results

For each fixed value of L (overhang distance in the potential plane), we are able to find the variation in the critical values F_U and F_L as γ changes. Then, in turn, we are able to use [3] to plot the separation angles. The $L = 1$ case is shown below, with the red/orange regions corresponding to λ_S values and blue/green regions corresponding to $\lambda_{S'}$ values.

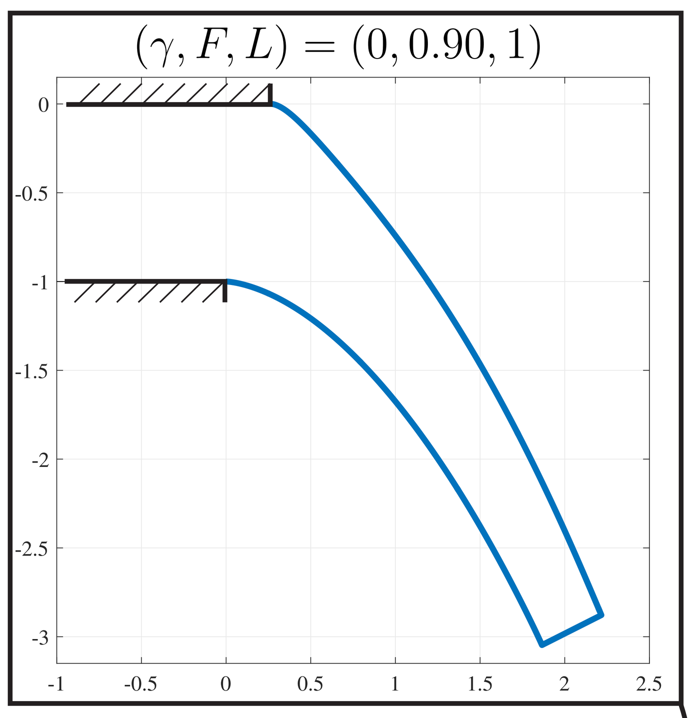

Fig. 2.1: Configuration with separation angles:
- $\lambda_S = \pi$ (tangential)
- $\lambda_{S'} = \pi$ (tangential)

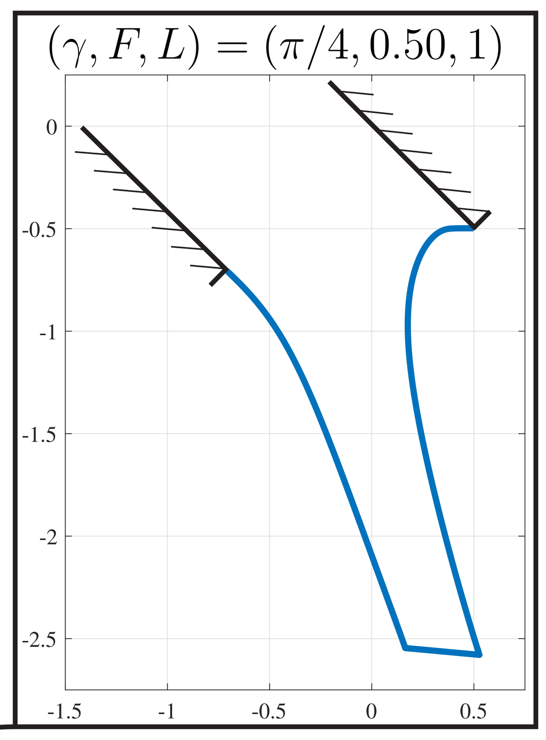

Fig. 2.2: Configuration with separation angles:
- $\lambda_S = \gamma$ (horizontal)
- $\lambda_{S'} = \pi$ (tangential)

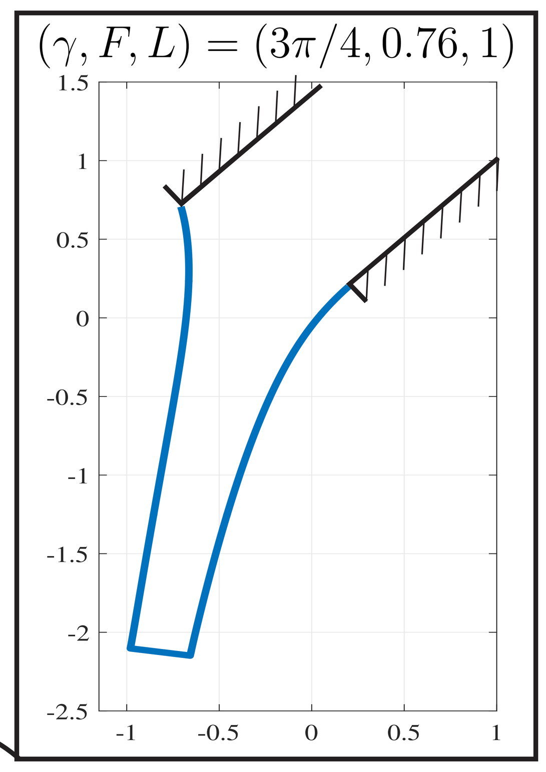

Fig. 2.3: Configuration with separation angles:
- $\lambda_S = \pi$ (tangential)
- $\lambda_{S'} = 2\pi/3$ (critical)

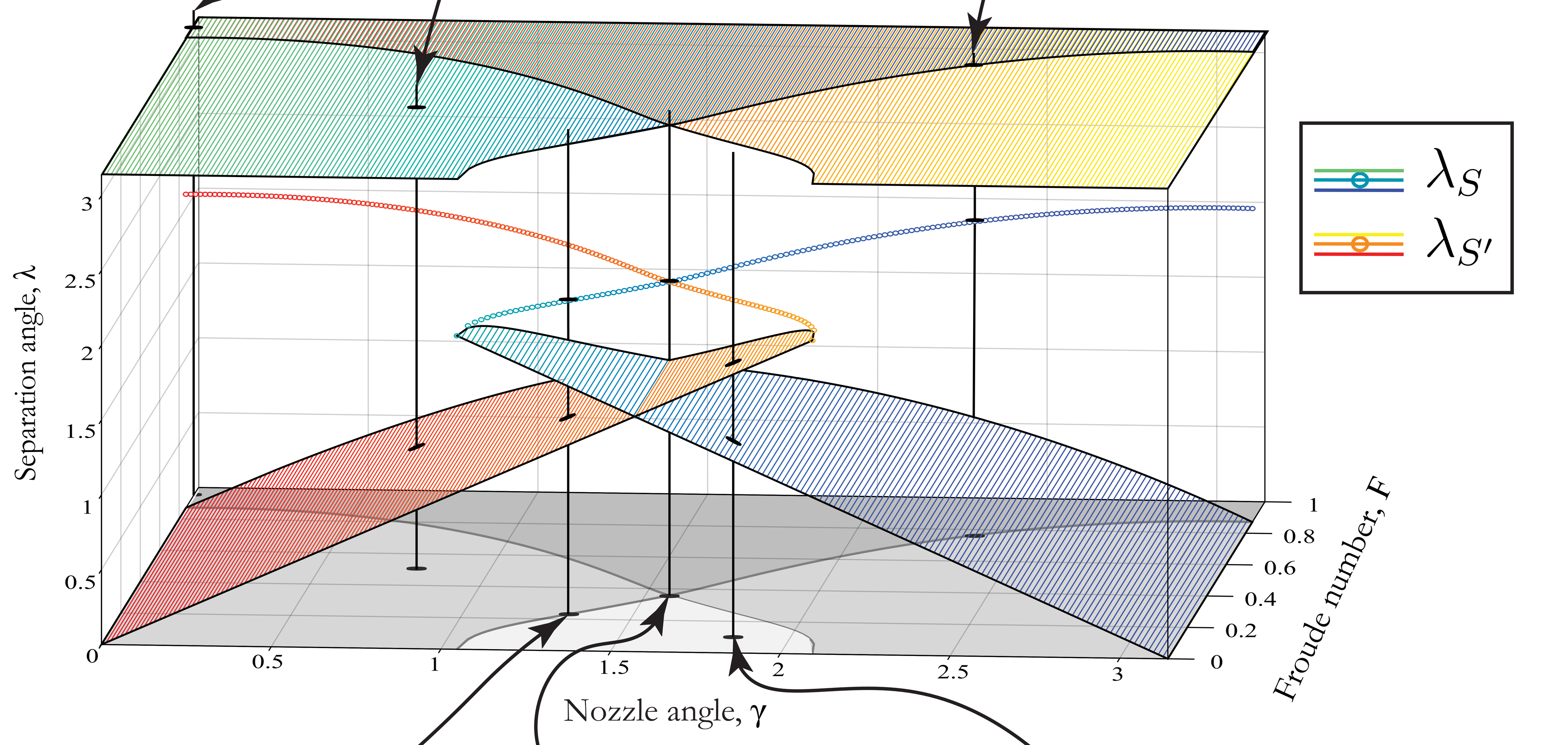

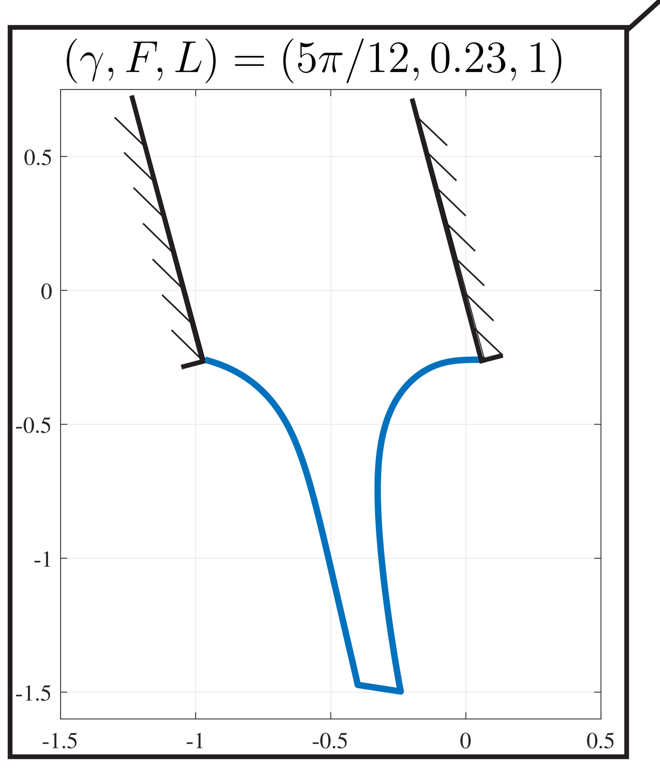

Fig. 2.4: Configuration with separation angles:
- $\lambda_S = \gamma$ (horizontal)
- $\lambda_{S'} = 2\pi/3$ (critical)

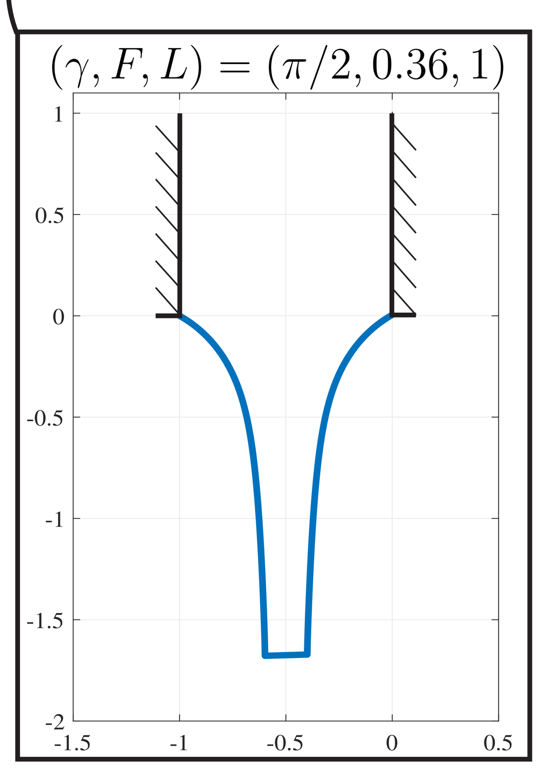

Fig. 2.5: Configuration with separation angles:
- $\lambda_S = 2\pi/3$ (critical)
- $\lambda_{S'} = 2\pi/3$ (critical)

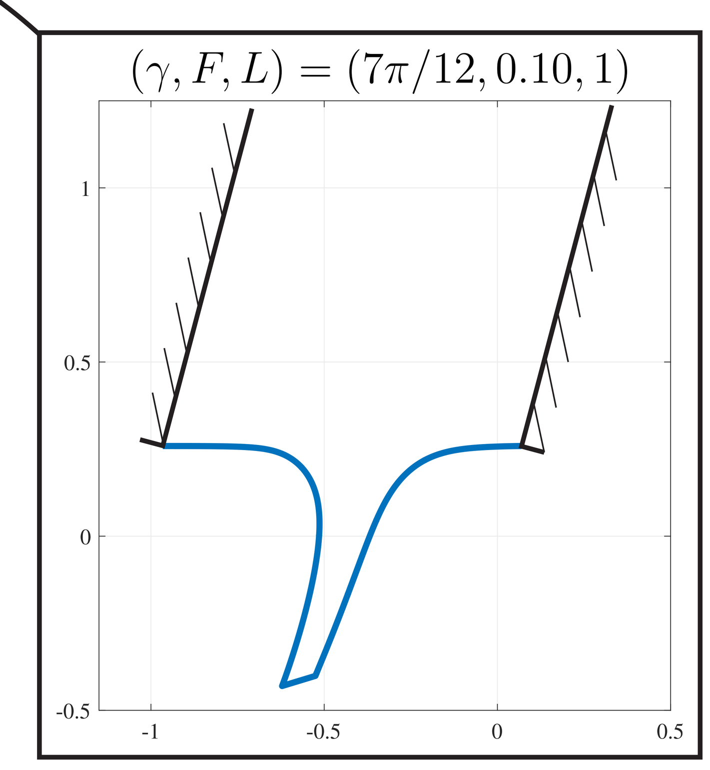

Fig. 2.6: Configuration with separation angles:
- $\lambda_S = \gamma$ (horizontal)
- $\lambda_{S'} = \gamma$ (horizontal)

Discussion

Our Fig. 2 serves as the main result of this work: by allowing for general nozzle inclinations, we are able to unify the previous horizontal and vertical formulations for a gravity-driven jet. Our work indicates how the separation angles for each surface depends on the chosen nozzle configuration and Froude number. Like the previous analyses, our numerical results indicate a critical Froude number (distinct for each surface) where the separation angle changes abruptly in the case of zero surface tension.

However, the situation is perhaps not as straightforward as it seems. Note that for each γ, a chosen L-value (the overhang length in the potential plane) is associated with a physical overhang, l, but only a *posteriori*. In an inverse manner, for a specified l-value, we are able to find a bounding Froude number, F_0, corresponding to a free-separation. It is furthermore found that if the Froude number is reduced, $F < F_0$, then the associated physical overhang must also reduce. The study of this 'back-flow' phenomenon is non-trivial due to the inverse nature of the formulation, but it raises the question of how the steady-states in this work are selected from a time-dependent model.

It is also found that the addition of surface tension into the model regularises the profile of the separation angles, thus allowing for a smooth transition from π to γ [see Chandler (2016) for more details]. This type of singular perturbative effect, due to small but finite surface tension, is reminiscent of the classic Saffman-Taylor viscous fingering problem; the asymptotic analysis of the $\alpha \to \infty$ limit for our jet-separation problem is the subject of ongoing work.

References

Chandler, T. (2016) "Jets, waterfalls and splashes from angled slots", BEE Extended Essay, University of Oxford, Internal Report.
Goh, K. and Tuck, E. (1985) "Thick waterfalls from horizontal slots", *J. Eng. Math.*, 19(4):341-349.
Vanden-Broeck, J.-M. (1984) "Bubbles rising in a tube and jets falling from a nozzle", *Phys. Fluids* **27**, 2601–2603.
Vanden-Broeck, J.-M. (2010) *Gravity-Capillary Free-Surface Flows*, Cambridge University Press.